Assessment of early demineralization in teeth using the signal attenuation in optical coherence tomography images

Dan P. Popescu
Michael G. Sowa
Mark D. Hewko
Lin-P'ing Choo-Smith
National Research Council of Canada
Institute for Biodiagnostics
435 Ellice Avenue
Winnipeg, Manitoba, R3B 1Y6
Canada

Abstract. Optical coherence tomography imaging is used to improve the detection of incipient carious lesions in dental enamel. Measurements of signal attenuation in images acquired with an 850-nm light source were performed on 21 extracted molars from eight human volunteers. Stronger attenuation was observed for the optical coherence tomography (OCT) signal in healthy enamel than in carious lesions. The measured attenuation coefficients from the two groups form distinct statistical populations. The coefficients obtained from sound enamel fall within the range of 0.70 to 2.14 mm^{-1} with a mean value of 1.35 mm^{-1}, while those in carious regions range from 0.47 to 1.88 mm^{-1}, with a mean value of 0.77 mm^{-1}. Three values are selected as the lower threshold for signal attenuation in sound enamel: 0.99, 0.94, and 0.88 mm^{-1}. These thresholds were selected to provide detection of sound enamel with fixed specificities of 90%, 95%, and 97.5%, respectively. The corresponding sensitivities for the detection of carious lesions are 92.8%, 90.4%, and 87%, respectively, for the sample population used in this study. These findings suggest that attenuation of OCT signal at 850 nm could be an indicator of tooth demineralization and could be used as a marker for early caries detection. © 2008 Society of Photo-Optical Instrumentation Engineers. [DOI: 10.1117/1.2992129]

Keywords: optical coherence tomography (OCT); enamel demineralization; incipient caries detection; light propagation in enamel.

Paper 08007R received Jan. 8, 2008; revised manuscript received May 15, 2008; accepted for publication Jul. 22, 2008; published online Oct. 6, 2008.

1 Introduction

In recent years, there has been a new focus in dental care that is evolving from the drilling and filling of cavities to nonsurgical management of early dental decay, clinically known as dental caries.[1] Incipient carious lesions (i.e., early lesions) are generally detected as white spots on the tooth enamel, and result from demineralization due to acid produced by bacteria in dental plaque. If left untreated, these lesions progress from the surface inward and eventually become cavitated. Treating lesions before they cavitate with agents such as fluoride can help to arrest the lesion, remineralize the site, and restore the enamel integrity. Successful nonsurgical management of caries requires an effective and objective method of detecting early lesions and monitoring their status. Traditional methods such as clinical radiography show poor sensitivity for detecting early carious lesions since the lesions are too shallow and do not provide enough contrast when compared with the surrounding tissue to be clearly discerned on a radiograph.[1] Furthermore, clinical inspection relying on visual examination and probing with a sharp dental explorer is a subjective

method depending on the examiner's experience and training. An intense effort to develop detection techniques that enable better diagnostic decisions has occurred in recent years. Most of the emerging diagnostic techniques are photonic technologies such as the DIAGNOdent and quantitative laser fluorescence (QLF) devices that are based on light- or laser-induced fluorescence spectroscopy. Despite their potential, these methods can generate false positive results due to stains, plaque, and food debris. These and other emerging methods have been reviewed in recent papers.[2,3]

Optical coherence tomography (OCT) is a candidate method for early caries detection. It is a technique that can accomplish with light what visual inspection and probing with a sharp dental explorer are designed to do but in a nonsubjective manner. The method is based on quantitative measurements of the backscattered light intensity as a function of depth into the region of interest, in this case the enamel layer of the tooth. It has been shown that this technique is well suited for detecting changes in optical scattering, tissue polarization, and refractive index due to morphological alterations within samples.[4,5] Previous reflectance measurements have indicated that demineralization and the accompanying biochemical and structural changes generate white spots in the

Address all correspondence to: Lin P'ing Choo-Smith, National Research Council of Canada, Institute for Biodiagnostics, 435 Ellice Avenue, Winnipeg, MB, R3B 1Y6 Canada. Tel: 204-984-7517; Fax: 204-984-5472; E-mail: linping.choo-smith@nrc-cnrc.gc.ca

enamel and demonstrate different local attenuation and scattering properties of light.[6] Also, our preliminary studies have found a good correlation between the OCT images of demineralized regions and the histological images of tooth sections cut from the respective lesion area.[7] This study focuses on the attenuation of the OCT signal in tooth enamel and explores its potential to be used as an objective quantitative parameter for distinguishing sound from carious enamel.

2 Materials and Methods

2.1 Tooth Samples

Tooth samples (21 human molars and premolars) were acquired from eight consenting patients at the University of Manitoba Dental Clinics who were undergoing extractions for orthodontic reasons. Following extraction, remaining soft tissue on the teeth was removed by scaling, and the samples were thoroughly rinsed with water. To avoid desiccation, the teeth were then preserved in sterile filtered deionized water until optical measurements. Each tooth sample was independently assessed *ex vivo* by two dental clinical investigators. Caries-free teeth had no visible decalcification or demineralization, while teeth with early carious lesions had regions of decalcification with intact surfaces and opacity of enamel that appeared as white spots when teeth surfaces were dry. The samples were used for OCT measurements without further treatment.

2.2 OCT System

OCT images were recorded with a Humphrey OCT-2000 system (Humphrey Systems, Dublin, California) as described previously.[8] Briefly, this system uses a superluminescent light-emitting diode (LED) with a central wavelength at 850 nm and a measured coherence length of ~15 μm [full width at half maximum (FWHM)] that provides the axial resolution of the OCT system. The transverse resolution, ~10 μm, is limited by the smallest rotation angle of the galvanometric mirror setup embedded in the system with the capability of steering the light beam into a succession of adjacent scans. In the reference arm, a rapid scanning optical delay line with a longitudinal free-space scan range of ~3 mm modulates the optical field. The resulting interferogram is digitized with a 16-bit A/D converter and demodulated. Two-dimensional images are formed by a straight-line collection of adjacent A-scans. Each OCT image consists of 100 A-scans, each scan being 500 pixels deep with a measured spatial resolution of 5.5×10^{-3} mm/pixel. The laser is focused to a thin line on the sample surface, with a total optical power of 750 μW for all image sets. The OCT-2000 system has an integrated camera for sample viewing and photographic acquisition during data collection. Samples were imaged in an upright position by affixing the apical root portion of the tooth to a microscope slide using dental rope wax.

2.3 OCT Image Acquisition and Processing

OCT images were collected from healthy enamel regions as well as from areas where incipient carious lesions were present. The images for this study were acquired from the proximal surfaces, i.e., the distal and mesial surfaces between adjacent teeth. Triplicate sets of images were obtained for each tooth surface from sound as well as carious enamel in order to ensure the experimental repeatability of measurements. A procedure was established in terms of sample positioning, normality of the scanned surface with respect to the probing beam, and OCT system parameters. This procedure ensured identical acquisition conditions of OCT images for all tooth samples examined. The white-light images from the integrated camera within our OCT-2000 system were also used to verify that the laser beam was always in focus across the regions scanned. The numerical aperture (NA) of the objective in the sample arm was calculated to be 0.036. This low numerical aperture is typical of OCT systems with fixed focus and ensures that the entire scan depth is within the focal zone. This experimental setup minimized the effect that focusing could have on the OCT signal intensity recorded along the probed distance within the sample.

An example of an OCT image from a caries-free area of a sample tooth is shown in Fig. 1(a). The image is corrected for the inherent curvature of the tooth surface by aligning the peak of the reflection rise occurring at the enamel/air interface in each A-scan along the same pixel horizontal line in the 2-D image. This 2-D OCT image (called a B-scan) consists of 100 A-scans such as the one shown by the dotted line in Fig. 1(b), which corresponds to the 13th depth line [leftmost dashed line in Fig. 1(a)]. As shown by the color map in the 2-D OCT image as well as by the A-scan in Fig. 1(b), the OCT signal decreases with the increase of light penetration in the tooth tissue.

Each A-scan corresponds to one position of the focused beam on the tooth surface, and the distance between adjacent A-scans is 20 μm. This generates B-scans that are 2 mm wide. Acquiring OCT images with small widths minimizes the impact of the surface curvature on the intensity of the recorded OCT signal across the section of interest. The noisy profile (dotted line) observed along the individual A-scan shown in Fig. 1(b) is due mostly to speckle noise. Speckle noise also manifests itself through the spotty pattern that can be observed across the 2-D image, and it is inherent to all systems that rely on interference for probing highly scattering samples. Multiple scattering of coherent light within the sample—in this case, the tooth matrix—generates speckle by forcing part of the light to experience a change in its travel distance relative to the initial ballistic path.[9,10] Quenching speckle noise as well as separating it from the "good" signal generated by light arriving at the detection system without being affected by multiple scattering events is necessary in order for the OCT measurements to provide a reliable assessment of highly turbid environments.

One method for speckle noise quenching is to sum (compound) OCT A-scans with uncorrelated speckle noise patterns.[11–15] In our case, since A-scans are acquired from adjacent spots located 20 μm apart on the tooth surface, the distribution of the scattering aggregates changes from one A-scan to another. Changing the distribution of scattering centers induces independent variations in the speckle pattern from one depth-scan to the next. Therefore, adding profiles of individual A-scans, each with its own particular noise pattern, will result in a smoother compounded depth profile, while reducing the speckle generated by multiple scattering of light as well as the noise generated by random electronic and thermal variations in the OCT detection system. As an example,
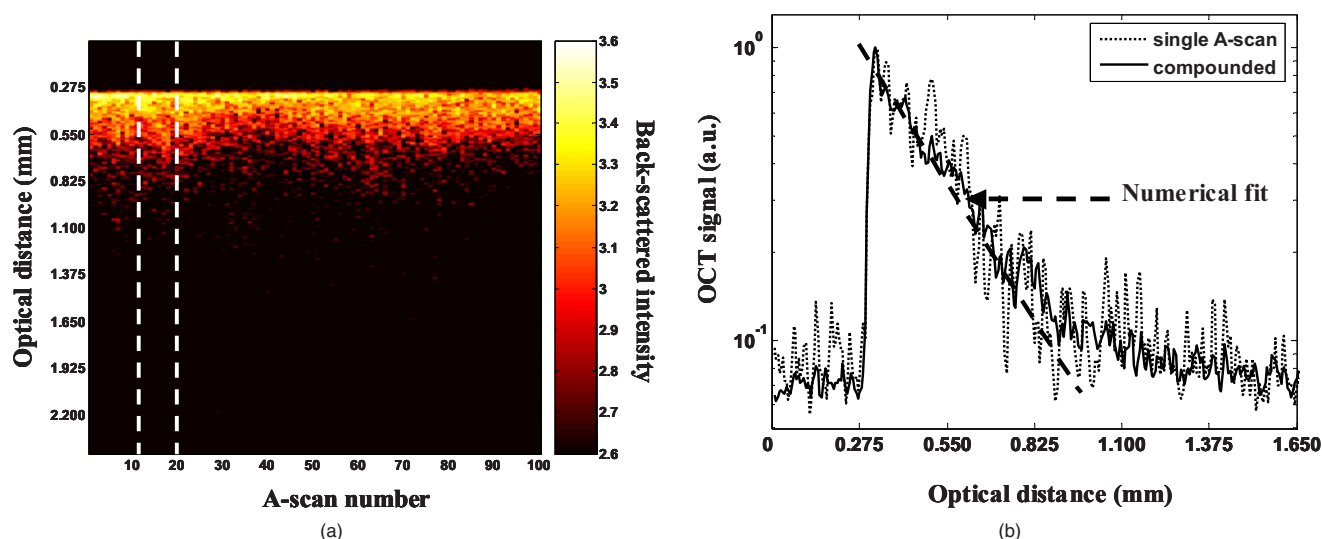
Fig. 1 (a) Example of a 2-D (B-scan) OCT image from healthy enamel. The two dashed lines bound the region contained between the 13th and the 20th A-scans. (b) The A-scan that corresponds to the 13th A-scan from (a). Shown are the single A-scan profile (dotted line) and the smoother profile obtained after adding (compounding) the eight adjacent A-scans, from the 13th up to the 20th A-scan (solid line). The exponential fit of the compounded profile follows the dashed line.

the compounded profile generated by adding eight adjacent A-scans, from the 13th up to the 20th scan, all contained within the region marked with dashed lines in Fig. 1(a), is represented by the solid line in Fig. 1(b). Both profiles are normalized with respect to the intensity of the reflection peak occurring at the air/enamel interface. The compounded profile is noticeably smoother when compared to the individual A-scan [dotted profile in Fig. 1(b)]. Importantly, an attenuation coefficient of the OCT signal penetrating the enamel matrix can be estimated for each compounded profile by fitting its curve with a Beer-Lambert-type function:[9]

$$I(z) \sim \exp(-2\mu z), \qquad (1)$$

where $I(z)$ represents the OCT signal intensity at an optical distance z beneath the tooth surface, and μ is the attenuation coefficient, the only parameter to be used for the numerical fit. The exponential numerical fit is represented in Fig. 1(b) by the dashed line.

As a general procedure, for each OCT image, three sets of eight adjacent A-scans each were selected at different locations within the image, and the A-scans from each set were co-added to generate a smoother attenuation profile. An attenuation coefficient was calculated for each profile by using numerical fits of the Beer-Lambert relation Eq. (1). In the carious regions, only the A-scans that were within the lesion were used for compounding.

2.4 Statistical Analysis

Attenuation coefficients determined from 522 OCT A-scans were grouped into those originating from sound or carious regions of enamel based on the consensus of independent examinations of each region by two dental clinical investigators. The sample population consisted of 345 attenuation coefficients associated with normal enamel and 177 coefficients from regions of caries. The mean and standard deviations from the mean were determined for both groups. Bootstrap

confidence intervals (CI) for the sensitivity of a test that uses the attenuation coefficient to distinguish caries from normal enamel were calculated using methods described by Platt et al.[16] The method selects a threshold that provides a fixed level of specificity, which signifies the ability of the test to distinguish sound enamel and determines the confidence level of the sensitivity of the test (ability to detect caries) at a fixed specificity using bootstrap resampling schemes. Both Wald-type and percentile bootstrap 95% confidence intervals of the sensitivity were determined using this method. Both intervals displayed similar coverage. The percentile bootstrap intervals are reported at thresholds for the test that fix the specificity at 75, 80, 85, 90, 95, 97.5, and 99%.

3 Results and Discussion

Two examples of compounded attenuation profiles of OCT signals at 850 nm as functions of optical penetration depth are presented in Fig. 2. One profile was obtained from a sound region, while the other characterizes OCT signal attenuation in a demineralized region. As can be observed, greater signal penetration and a lower attenuation of the 850-nm OCT signal, corresponding to a smaller slope for the exponential fit, is obtained in the demineralized region when compared to attenuation obtained in sound enamel. This difference in signal attenuation can therefore be potentially used as a marker to identify incipient demineralization volumes beneath otherwise intact tooth surfaces.

To investigate this possibility, a total of 522 attenuation coefficients were extracted from the available OCT images. The OCT signal attenuation for 345 measurements of sound enamel on 42 surfaces from 21 tooth samples ranged from 0.70 to 2.14 mm^{-1}, with a population mean value of 1.35 mm^{-1} and a standard deviation (sd) of 0.28 mm^{-1}. Another set of 177 measurements on surfaces identified as presenting early carious lesions were acquired from 23 surfaces spread among 16 teeth and display lower values for signal
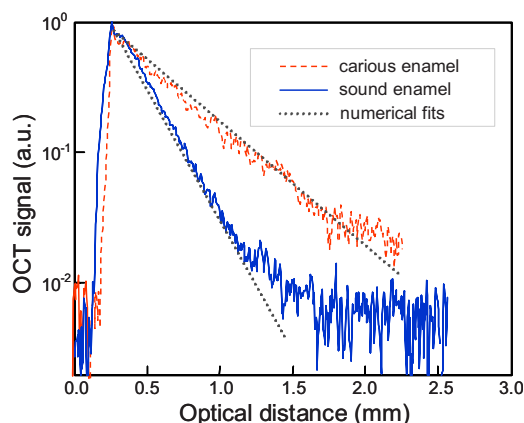
Fig. 2 Compounded profiles representing the magnitude of the OCT signal as a function of the optical penetration depth within the enamel in a sound and an incipient demineralization case together with their respective numerical fits on a logarithmic scale.
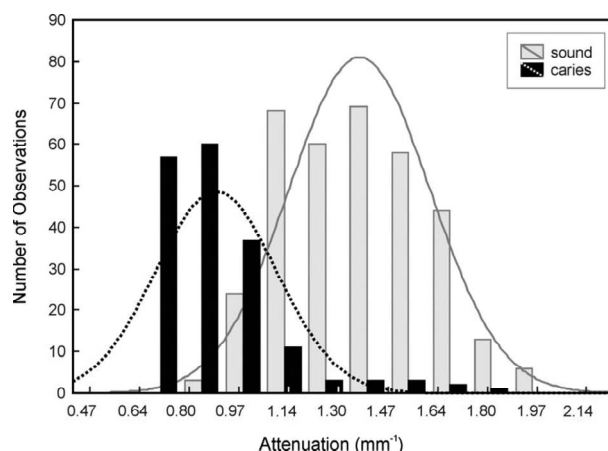

Fig. 3 Histograms of the attenuation coefficients obtained for the 850-nm OCT signal corresponding to healthy and demineralized enamel. The normal distribution fits are also shown.

attenuation at 850 nm with coefficients ranging from 0.47 to 1.88 mm^{-1}, with a mean (sd) population value of 0.77 (0.24) mm^{-1}. These numbers are also summarized in Table 1. The population means between the sound and carious regions of enamel were statistically significantly different at $p < 0.05$. Histograms of the two populations along with the normal distribution fits as a function of the optical attenuation coefficient at a wavelength of 850 nm are presented in Fig. 3. The sensitivity of using the attenuation coefficient to detect caries is ascertained at a series of thresholds that convey different specificities, thus assessing the ability of the method to detect sound enamel. The results of the statistical analysis for seven threshold values are summarized in Table 2. Clearly, there is a trade-off between sensitivity and specificity of the test, with the sensitivity of the test going down as the threshold is varied from 1.12 to 0.81 mm^{-1}. The two distributions cross at approximately 1.0 mm^{-1}, suggesting that the optimal threshold that would separate the two populations with the fewest false positives and false negatives is localized around this value. Therefore, by using the value of 0.99 mm^{-1} as a diagnostic threshold for caries, 39 of the 345 measurements on sound enamel would be misclassified as caries, while 20 of the 177 measurements on caries are misclassified as sound.

This translates into values for the sensitivity and specificity close to 90%, proving that the optical attenuation coefficient of the OCT signal at a wavelength of 850 nm in enamel could be used as a clinical marker for early caries detection.

The trend was very clear in every case where a demineralization spot was available and compared with sound areas on the same tooth. OCT signal attenuation in healthy enamel is higher than the attenuation while propagating within a lesion. Thus, when using OCT at 850 nm as a method to screen for early caries lesions by scanning over a tooth surface looking for areas of anomalously low optical attenuation, one might expect improved sensitivity and specificity over conventional detection methods such as radiographs and visual inspection.

OCT images (B-scans) of sound and carious enamel collected from the distal surface of one tooth sample are shown

Table 1 Summary of the sampling numbers used in the statistical analyses of the optical attenuation coefficient values obtained from OCT images at 850 nm.

	Sound	Caries
# of teeth	21	16
# of surfaces	42	23
# of measurements	345	177
Mean attenuation (mm^{-1})	1.35	0.77
Std. dev.	0.28	0.24
Attenuation range (mm^{-1})	0.70–2.14	0.47–1.88

Table 2 Percentile bootstrap confidence intervals (CI) for the sensitivity at a fixed level of specificity of a diagnostic test based on using the OCT attenuation coefficient derived from the analysis of OCT A-scans. Results of the statistical analysis of the optical attenuation coefficients obtained by using seven different thresholds are displayed.

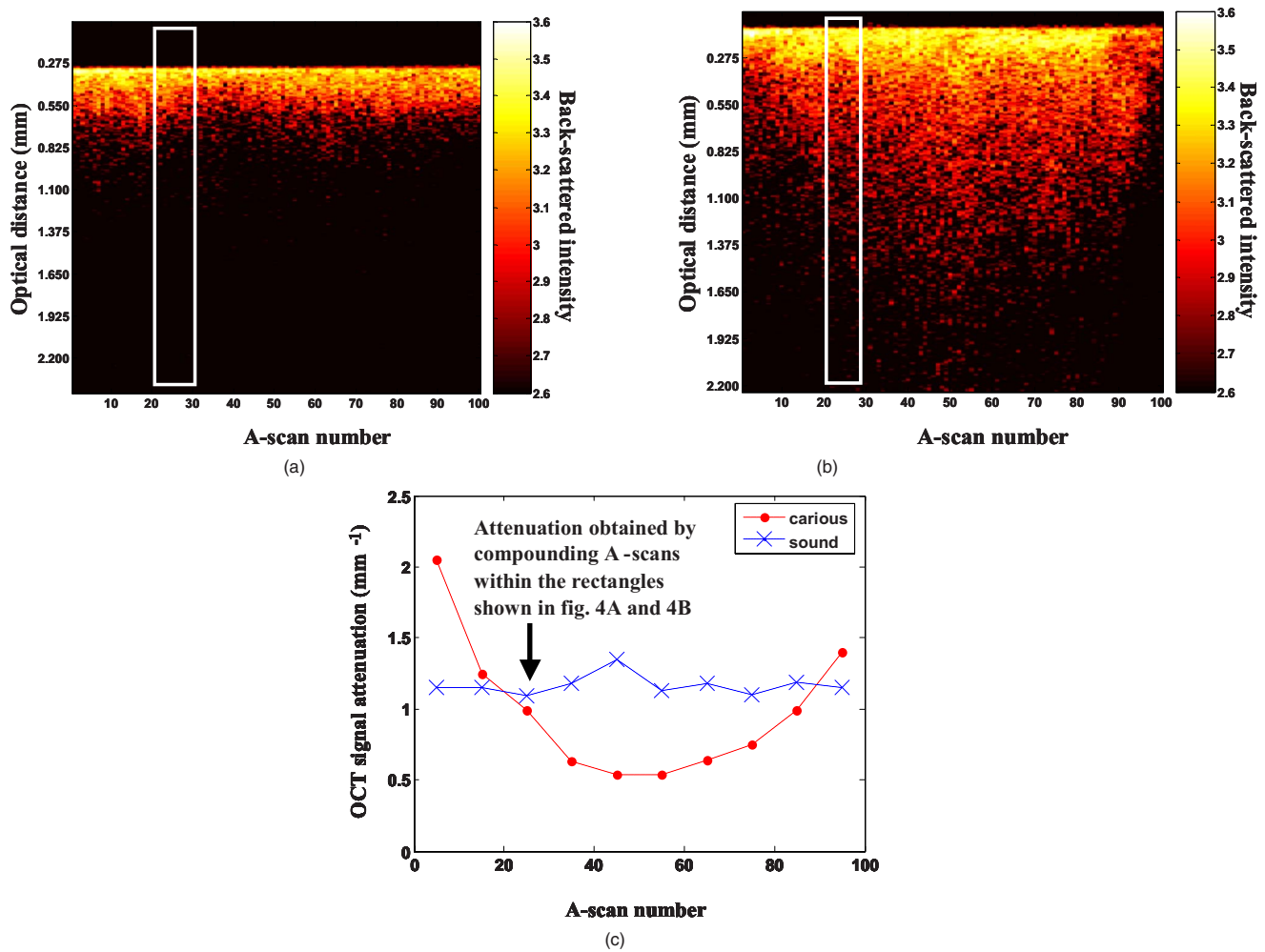| Fixed Specificity	Threshold for OCT Attenuation (mm^{-1})	Sensitivity	
		Lower 95% [CI]	Upper 95% [CI]
75%	1.12	88.9%	96.6%
80%	1.08	87.2%	95.8%
85%	1.04	85.3%	94.8%
90%	0.99	82.9%	92.8%
95%	0.94	77.3%	90.4%
97.5%	0.88	67.2%	87.0%
99%	0.81	51.9%	82.2%

(a)

(b)

(c)

Fig. 4 OCT images of (a) sound enamel and (b) a demineralized region located on the same tooth. As an example of the procedure, the 21st to the 30th A-scans in (a) and (b) are shown within rectangles in both figures and are compounded to yield the corresponding attenuation coefficients [arrow in (c)]. (c) Distribution of the attenuation coefficient values in the sound region (×), and across the carious lesion (●). The connecting lines are for guidance only.

in Figs. 4(a) and 4(b), respectively. For sound enamel, there is at first an intense backscattered signal at the air/enamel interface, with the rest of the signal that propagates along the initial direction rapidly decaying with increasing depth into the sample. With carious lesions, there is a relatively similar intense reflection rise at the initial interface; however, in contrast to sound enamel, there is significantly more signal backscattering with depth beyond the surface. As explained earlier, a lower OCT signal attenuation for an incipient lesion translates into acquiring an OCT signal generated by light that travels longer within the tooth matrix, as can be clearly seen in Fig. 4(b), when compared to a signal that travels through healthy enamel [Fig. 4(a)]. While light is strongly scattered by the relatively well-ordered rod structure that characterizes sound enamel, its propagation is complicated by the addition of new structures within the volume of a lesion. In addition to nonaltered rods, incipient lesions contain regions with various degrees of mineral loss and a multitude of pores of different sizes.[17,18] When penetrating through such a complex structure, in addition to scattering by intact enamel rods, light experiences additional interaction with the pores. There are two

types of light-demineralization pore interactions, each resulting in greater light intensity being sent toward the detection system when compared to the signal obtained in the sound case. First, there are the back reflections occurring at the pore/enamel interfaces due to abrupt changes of the optical refractive index. Second, there is an effective reduction in scattering when light is traveling virtually without being deviated through the space inside the pores. This effect ensures that light coming from deeper within the sample reaches the OCT detection system. As observed when comparing Fig. 4(a) with Fig. 4(b), the final result of these two processes amounts to more OCT signal being recorded as arising from deeper within the carious enamel matrix compared to a signal that probes sound enamel and does not penetrate too deep into the sample.

In order to examine the signal attenuation across the full width of 100 A-scans in these two OCT images, the images were partitioned into 10 sections, each section containing 10 A-scans that were compounded, and the resulting profile was numerically fitted to relation (1) in order to generate an attenuation coefficient value corresponding to each partition. As
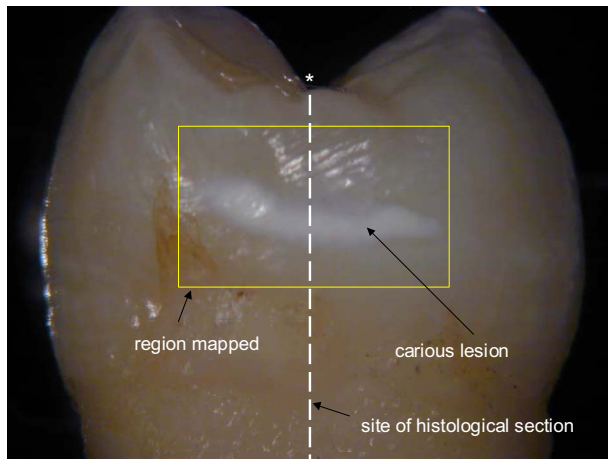
Fig. 5 Photograph of the distal surface of an extracted human premolar that shows a demineralized region or "white spot." The asterisk at the crown serves for orientation purposes for Fig. 7.

an example of the procedure, the sections that include all the A-scans from the 11th scan up to the 20th scan are marked with rectangles in Figs. 4(a) and 4(b) and their corresponding attenuation values, indicated by an arrow, are plotted in Fig. 4(c). As shown in Fig. 4(c), the OCT signal attenuation coefficients are mostly constant, with values around 1.20 mm^{-1}, across the region of the sampled sound enamel (values connected for guidance by the dotted line). In contrast, starting from the sound edges of the demineralization region [Fig. 4(b)], where attenuation values indicate sound enamel, smaller values for the OCT attenuation signal are found while progressing toward the center of the figure, therefore indicating a region with incipient demineralization.

The spatial change in optical attenuation at 850 nm is further explored by acquiring a series of 14 parallel OCT images at 200-μm intervals across the distal surface of an extracted human premolar containing an incipient carious lesion and shown in the white-light photograph in Fig. 5. The overall scanned region is outlined by the rectangle included in the photograph. Similar to the method described earlier and applied to generate Fig. 4(c), series of 10 attenuation coefficients were extracted from each OCT image belonging to a group of 14 B-scans acquired at 200-μm intervals across the demineralization spot from within the rectangular area shown in Fig. 5. All of the attenuation values are projected onto a 2-D map in Fig. 6(a) that spatially matches the region from within the rectangle in Fig. 5. Each attenuation value represented in Fig. 6(a) could be treated as an average result obtained for the OCT signal propagation occurring across a 200×200 μm^2 area on the tooth surface. A comparison with the white-light photograph (Fig. 5) shows that low OCT signal attenuation coefficients [darker regions in Fig. 6(a)] match the carious regions, while high attenuation coefficients correspond to sound enamel. It is observed that the attenuation values at the edges map out a slightly larger lesion size than that shown in the photograph. This likely indicates that the method is also able to identify the shallower demineralization regions that are expected to occur at the periphery of a lesion site but that are not yet discernible by visual inspection. This hypothesis was validated through histology and Raman spec-

troscopy in our previous publications.[7,8] These methods also confirmed that the small spot located in the middle of the top edge in Fig. 6(a) is not the result of demineralization. This false positive is the result of an experimental artifact introduced into the OCT measurements by the curvature of the tooth surface. It is expected that such artifacts can be eliminated when measurements are performed with an OCT probe head that has the laser beam oriented orthogonal on the tooth surface.

A series of decision thresholds determined from the statistical analysis of the attenuation coefficients calculated from an independent sample population are applied to segment the 2-D image of the OCT attenuation coefficient [Fig. 6(a)] over the area of the tooth presented in Fig. 5. Binary segmentation of the 2-D map of the determined OCT attenuation coefficients using thresholds of 0.99, 0.94, and 0.88 mm^{-1} are presented in Figs. 6(b)–6(d). Black regions of the binary image correspond to locations where the OCT signal attenuation is smaller than the threshold value and associated with caries, while white covers the areas with attenuation higher than the threshold and corresponds to sound enamel. The black area in the middle of the binary representation resembles the shape of the white spot identified visually in Fig. 5. As the threshold used to impose the binary segmentation of the attenuation image is decreased, the total area identified as carious decreases. Examining this series of binary images graphically illustrates the utility of using a few different binary segmentation thresholds to visually distinguish areas of the tooth that are mostly likely carious and to help eliminate false positives.

As a validation for the analysis performed in connection with Fig. 5 and Figs. 6(a)–6(d), Fig. 7 displays a photomicrograph of a transverse thin tooth section (~115 μm) obtained from the position corresponding to the location marked by the dashed line in the photograph. The carious lesion can be clearly distinguished as a dark region located at the top of the histological image.

4 Conclusions

Our studies have established the basis of an objective method of differentiating healthy enamel from incipient carious enamel based on light attenuation of the OCT signal at 850 nm. A number of OCT measurements on healthy and demineralized enamel were systematically acquired and compared. The total attenuation coefficient of OCT signal within the tooth is a parameter that quantifies the interaction between light and tooth matrix. We have demonstrated that the signal attenuation is a quantity sensitive to tooth demineralization occurring beneath tooth surfaces and therefore could be used as a marker for detecting incipient demineralization. Also, it was shown that the 850-nm OCT signal is attenuated less in carious enamel than in sound enamel. This is likely due to two concurring effects generated by the presence of pores as a result of the demineralization process. First, due to lack of scattering centers inside the demineralization pores, light travels unperturbed through the pore volume, so less light intensity escapes from the optical field of view of the collimating lens and/or from the spatial coherence gate of the OCT system as it penetrates the carious tissue than when traveling an equivalent distance in sound enamel. Second, stronger back reflections occurring at the enamel/pore interfaces in the cari-
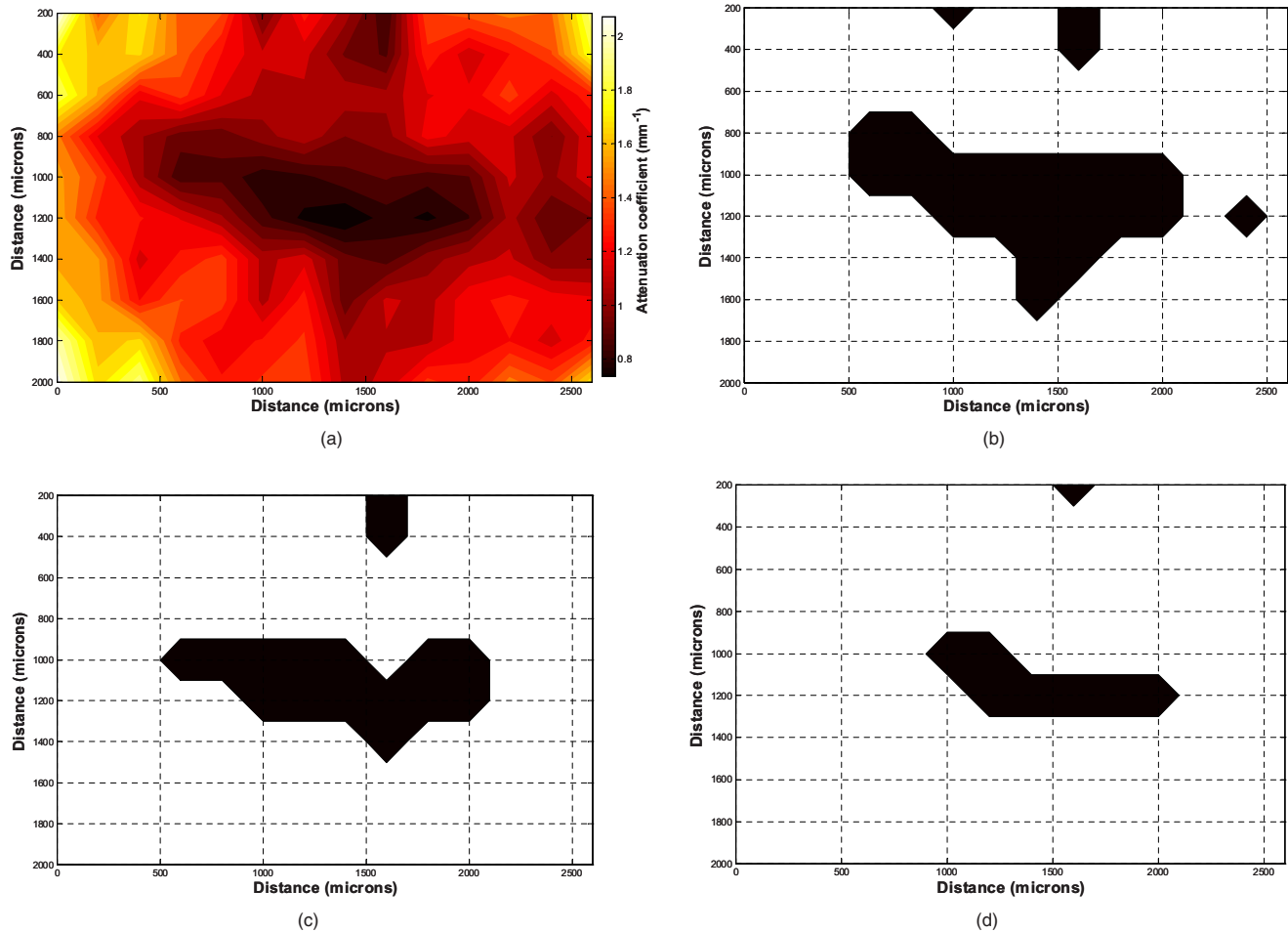
(a)

(b)

(c)

(d)

Fig. 6 (a) Two-dimensional mapping of the OCT attenuation coefficient values across the area marked by a rectangle in Fig. 5. (b) Binary image of the attenuation values from panel (a), with white marking the areas with higher attenuation than the threshold value of 0.99 mm^{-1}, while black corresponds to regions where the OCT signal attenuation is smaller than the threshold value. (c) Binary image similar to (b) but with the threshold value set at 0.94 mm^{-1}. (d) Binary image with the threshold attenuation coefficient set at 0.88 mm^{-1}. The specificities and sensitivities corresponding to these three thresholds are displayed in Table 2.

ous case send more signal intensity back toward the detection system from deeper within the tooth matrix. The cumulative action of these two processes reduces the effective attenuation of the OCT signal when measured in carious tissue. Since OCT technology can be readily coupled with fiber-optic technology for delivering light to the sample (i.e., patient's tooth) and collecting the backscattered light for analysis, OCT is a good candidate as a potential clinical tool for guiding the

detection and monitoring of teeth in the early stages of demineralization. The promising results obtained in these studies are an incentive for more extensive validation studies containing larger sample sets. Studies that involve the cross-correlation of results obtained from the noninvasive method of OCT imaging of unsectioned samples with the current gold standard method of transverse microradiography on tooth histological sections are also underway.
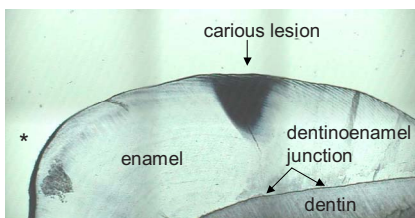

Fig. 7 Photomicrograph of the histological section obtained from the plane marked by the dashed line in Fig. 5. The thickness of the histological section is 115 μm. The asterisk at the crown is marked for reference to Fig. 5.

References

1. National Institutes of Health, "Diagnosis and management of dental caries throughout life; National Institutes of Health Consensus Development Conference statement, March 26–28, 2001," *J. Dent. Educ.* **65**, 1162–1168 (2001).

2. A. Hall and J. M. Girkin, "A review of potential new diagnostic modalities for caries lesions," *J. Dent. Res.* **83**, C89–C94 (2004).

3. G. K. Stookey and C. Gonzalez-Cabezas, "Emerging methods of caries diagnosis," *J. Dent. Educ.* **65**, 1001–1006 (2001).

4. R. K. Wang and V. V. Tuchin, "Optical coherence tomography—light scattering and imaging enhancement," Chapter 13 in *Handbook of Coherent Domain Optical Methods*, Vol. **2**, V. V. Tuchin, Ed., pp. 3–60, Kluwer Academic Publishers, Boston (2004).

5. D. Fried, J. Xie, S. Shafi, J. D. Featherstone, T. M. Breunig, and C. Le, "Imaging caries lesions and lesion progression with polarization sensitive optical coherence tomography," *J. Biomed. Opt.* **7**, 618–627 (2002).

6. C. Mujat, M. H. van der Veen, J. L. Ruben, J. J. ten Bosch, and A. Dogariu, "Optical path length spectroscopy of incipient caries lesions in relation to quantitative light-induced fluorescence and lesion characteristics," *Appl. Opt.* **42**, 2979–2986 (2003).

7. M. D. Hewko, L.-P. Choo-Smith, A. C.-T. Ko, L. Leonardi, C. C. S. Dong, B. Cleghorn, and M. G. Sowa, "OCT of early dental caries: a comparative study with histology and Raman spectroscopy," in *Lasers in Dentistry XI*, P. Rechmann and D. Fried, Eds., *Proc. SPIE* **5687**, 16–24 (2005).

8. M. G. Sowa, D. P. Popescu, J. Werner, M. D. Hewko, A. C.-T. Ko, J. Payette, C. C. S. Dong, B. Cleghorn, and L.-P. Choo-Smith, "Precision of depolarization and optical attenuation measurements of sound tooth enamel," *Anal. Bioanal. Chem.* **387**, 1613–1619 (2007).

9. J. M. Schmitt, A. Knüttel, M. Yadlovski, and M. A. Eckhaus, "Optical-coherence tomography of a dense tissue: statistics of attenuation and scattering," *Phys. Med. Biol.* **39**, 1705–1720 (1994).

10. B. Karamata, M. Laubscher, M. Leutenegger, S. Bourquin, T. Lasser, and P. Lambelet, "Multiple scattering in optical coherence tomography. I. Investigation and modeling," *J. Opt. Soc. Am. A* **22**, 1369–1379 (2005).

11. J. M. Schmitt, "Array detection for speckle reduction in optical coherence microscopy," *Phys. Med. Biol.* **42**, 1427–1439 (1997).

12. M. Bashkansky and J. Reintjes, "Statistics and reduction of speckle in optical coherence tomography," *Opt. Lett.* **25**, 545–547 (2000).

13. D. P. Popescu, M. D. Hewko, and M. G. Sowa, "Speckle noise attenuation in optical coherence tomography by compounding images acquired at different positions of the sample," *Opt. Commun.* **269**, 247–251 (2006).

14. A. I. Kholodnykh, I. Y. Petrova, K. V. Larin, M. Motamedi, and R. O. Esenaliev, "Precision of measurement of tissue optical properties with optical coherence tomography," *Appl. Opt.* **42**(16), 3027–3037 (2003).

15. K. V. Larin, M. G. Ghosn, S. N. Ivers, A. Tellez, and J. F. Granada, "Quantification of glucose diffusion in arterial tissues by using optical coherence tomography," *Laser Phys. Lett.* **4**(4), 312–317 (2007).

16. R. W. Platt, J. A. Hanley, and H. Yang, "Bootstrap confidence intervals for the sensitivity of a quantitative diagnostic test," *Stat. Med.* **19**(3), 313–322 (2000).

17. P. Ngaotheppitak, C. L. Darling, and D. Fried, "Measurement of the severity of natural smooth surface (interproximal) caries lesions with polarization sensitive optical coherence tomography," *Lasers Surg. Med.* **37**, 78–88 (2005).

18. C. Robinson, R. C. Shore, S. J. Brookes, S. Strafford, S. R. Wood, and J. Kirkham, "The chemistry of enamel caries," *Crit. Rev. Oral Biol. Med.* **11**, 481–495 (2000).